

Keep the Material Model simple with input from Elements that predict the Correct Deformation Mode

T. Tryland¹, T. Berstad²

¹SINTEF Raufoss Manufacturing, Raufoss, Norway

²Department of Structural Engineering, Norwegian University of Science and Technology, Trondheim, Norway

1 Background

The 64 km/h frontal offset test is run with a deformable barrier, and the first numerical model of this barrier was made with solid elements to represent the honeycomb blocks. However, this required development of a special element formulation to handle the severe deformation of the solid elements together with a special material model that could be calibrated to handle the extreme anisotropy [1]. It is herein important to notice the amount of work, the uncertainties with the test specimens and the test procedure to get a proper representation of the honeycomb material. It was therefore suggested to represent the barrier geometry with shell elements that were able to capture the deformation mode with local and global buckling of the honeycomb structure together with a simple model to represent the material in the 0.076 mm thick aluminium foil [2]. The objective of this study was to investigate whether the same idea can be used to predict cracks when crushing a two chamber aluminium profile.

2 Specimen geometry and test procedure

Note that the component that was tested in this study is unlike the situation for real products where the actual combination of geometry and material have to secure robust behaviour for all combinations within the tolerances. Here a combination of profile geometry, cutting angles, wall thicknesses and material properties was chosen to get an unstable folding pattern and thereby challenge the simulation tool to capture this. The results from the parallel tests shown in Figure 1 confirm large variation when comparing parallel tests.



Fig. 1: Parallel tests show specimen 2, 4 and 6 that does not follow progressive folding.

The tests were run in a large quasi-static press where the loading was applied sufficiently slowly to avoid dynamic effects. The definition of the cut angles to initiate axial folding from the top was found in the literature [3], but in this example the profile geometry was chosen with a relatively thin mid-wall to challenge the material locally in the two corners between the outer skin and the mid-wall. The result was a profile that behaves unstable in this crushing test [4], see Figures 1 and 2. It was therefore interesting to investigate whether this mid-wall represents sufficient stiffness to control the folding mode when the outer part of the profile behaves unstable due to geometrical imperfections.

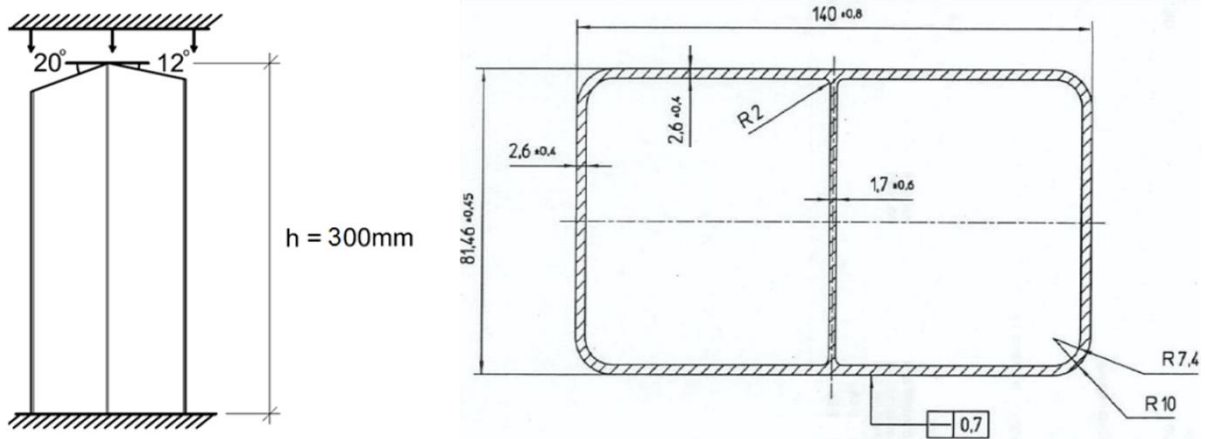


Fig.2: Definition of profile geometry and specimen with cut angles to initiate axial folding [4].

3 Convergence gives no guarantee that the correct solution is found

Finite element simulations can be a useful design tool when the code has proved correct predictions. But misleading results should be avoided, and structural engineers often use hand calculations to effectively evaluate the critical details. This often means use of analytical expressions that are developed for the actual design challenge where good understanding of the interaction between geometry and material is required to formulate proper equations based on relevant simplifications [5]. An impressive amount of work has been performed to investigate and test relevant structural designs, and the load bearing capacity is formulated as design codes where BS 8118 [6] and Eurocode 9 [7] are well known examples for aluminium. Remember that the user-friendliness and the complexity in these design formulas should be a balance between how many details can be included before the equations get so extensive that the risk for mistakes becomes too high.

Finite element simulations can be an alternative to analytical expressions for complex structures. The base for FEM simulations is that a complex geometrical challenge can be divided into simpler tasks. This has shown to be a good design tool when used correctly. It is important to notice that it is clearly written in the output file that the code owner has no responsibility for the validity, accuracy or applicability on any results obtained from the simulation, and the user must verify his own results. Therefore, it is likely that even if the current software for finite element simulations does not require user competence that includes any understanding of the interaction between geometry and material, this is beneficial to be able to use this software effectively as a design tool. The idea here is that the elements handle the deformation mode, and the material model has to handle the phenomena related to metallurgical explanations, see Figure 3.

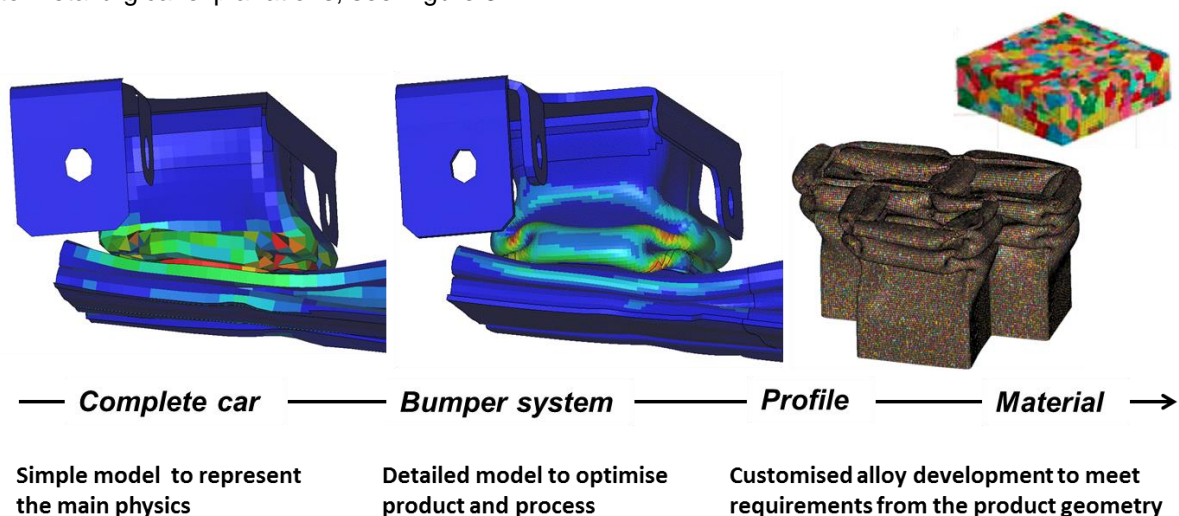


Fig.3: Different phenomena and detailing when predicting the correct deformation mode.

This means a strong focus to find the combinations of element type and element meshes that seem able to predict the correct deformation mode that could be relevant both at a global and a local level. It is likely that different element sizes and levels of detailing are required to capture the different physical phenomena with their strain- and stress components as input to an engineering fracture model for the structural component and a detailed fracture model for the material test specimen. The material model can then be kept as simple as possible where the ductility is seen as a material constant. This means that inverse modelling with the shear specimen [8], or other geometries that are used to measure ductility, should be performed with an element mesh that predict both convergence and correct deformation mode at a detailed level [9]. Remember that every node has a stiffness related to its movement in the three directions, and these stiffness components may be affected by the element type, the element size and the element orientation. The different element formulations have different simplifications that have minor influence in some cases, while they may be not acceptable in other cases where refining the mesh does not solve the challenge. This is illustrated in Figure 4 where the circumference of a circle with diameter D is calculated numerically. The "linear" method at left hand side starts with the blue quadrat where the segments summarise to $4D$. The green one subtracts a new quadrat in each corner, while the red one subtracts even more quadrats to get closer to the circle. This process can be continued until the numerical representation looks like a circle. However, the sum of the segments is $4D$ for all alternatives illustrating that not even the immediate convergence in this example can guarantee that the correct solution is found. The segments are kept either horizontal or vertical, and one important issue with the circle is not represented by this.

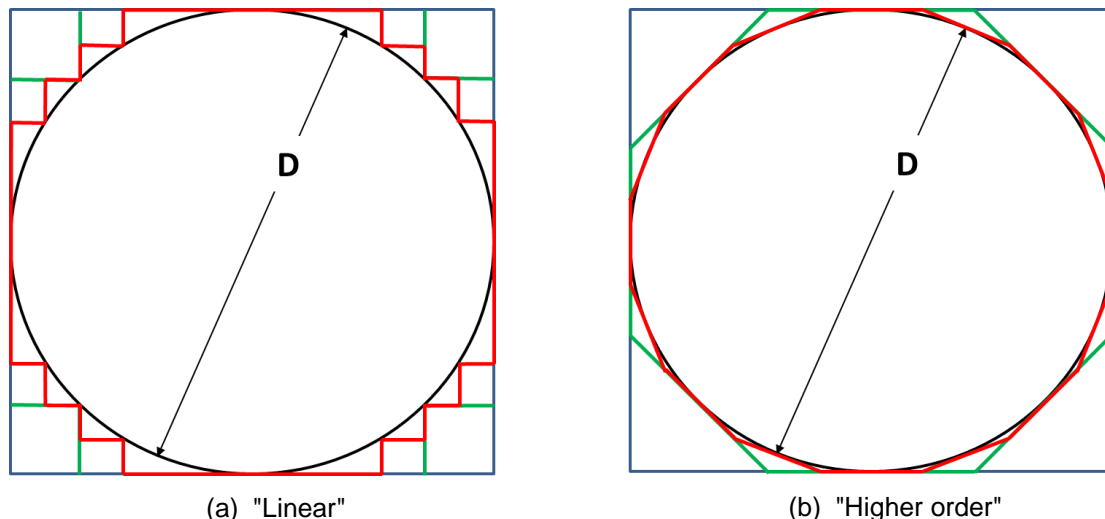


Fig.4: An illustration of two numerical approaches to calculate the circumference.

The "higher order" alternative takes into account the varying slope as one important feature for the circle. This requires a more comprehensive formulation for the length of each segment, but the benefit is $4D$ for the blue quadrat followed by $3.31D$, $3.18D$, $3.15D$, $3.144D$, $3.1422D$, $3.14175D$... It is worth noticing that even these calculations are simple when the tangent function is known, and the results show convergence towards the value π times D as expected. It is also shown that the convergence is relatively fast as the mistakes by the green and red segments are just above 5 % and 1 %, respectively. It seems crucial to capture these important features, and with this analogy it could be an idea to prioritise more accurate elements instead of a refined mesh with the simplest ones.

The objective of this study was to investigate how to keep the material model simple with input from elements that predict the correct deformation mode. The Cockcroft-Latham parameter is then seen as a material constant where the critical value requires that the mesh is sufficiently fine. As illustrated in Figure 3, this should be the case when modelling the crushing test for customised alloy development to meet the requirements from the product geometry. Moreover, the detailed model to optimise product and processes should not be too far from this situation, while the simple model to represent the main physics is likely to be so far away from convergence that eventual fracture predictions have to be made with reduced values that are calibrated with experiments or more detailed FEM models. However, practical engineers may still find this coarse approach useful as it is sufficiently fast, and elements with aspect ratio like 4 were therefore included as the coarsest alternative in this study.

4 Shell and solid elements with aspect ratio about 4

The specimen geometry that was used when crushing the two chamber profile was represented by both shell and solid elements with aspect ratio about 4 to predict the correct deformation mode [9]. These alternatives may be useful for the practical engineer as they are fast enough to fit inside for example complete car simulations. Note that this means about one million elements to represent 50 square meters of plates with average thickness 1.8 mm. It is also worth remembering that this starting point illustrated at the left hand side in Figure 5 will require either shell elements or solid elements with **ELFORM** equal to minus 2 [10]. Smaller solid elements can be used to achieve a better description of the deformation mode, while smaller shell elements are questionable as the predicted deformation is too localized to the corners compared with the test results. It is also shown that smaller shell elements than four times the thickness increase the tendency for local buckling at the expense of global buckling [9]. A numerical model with small shell elements may predict axial folding of a member that is so long that the test result shows dramatically less energy absorption due to global buckling.

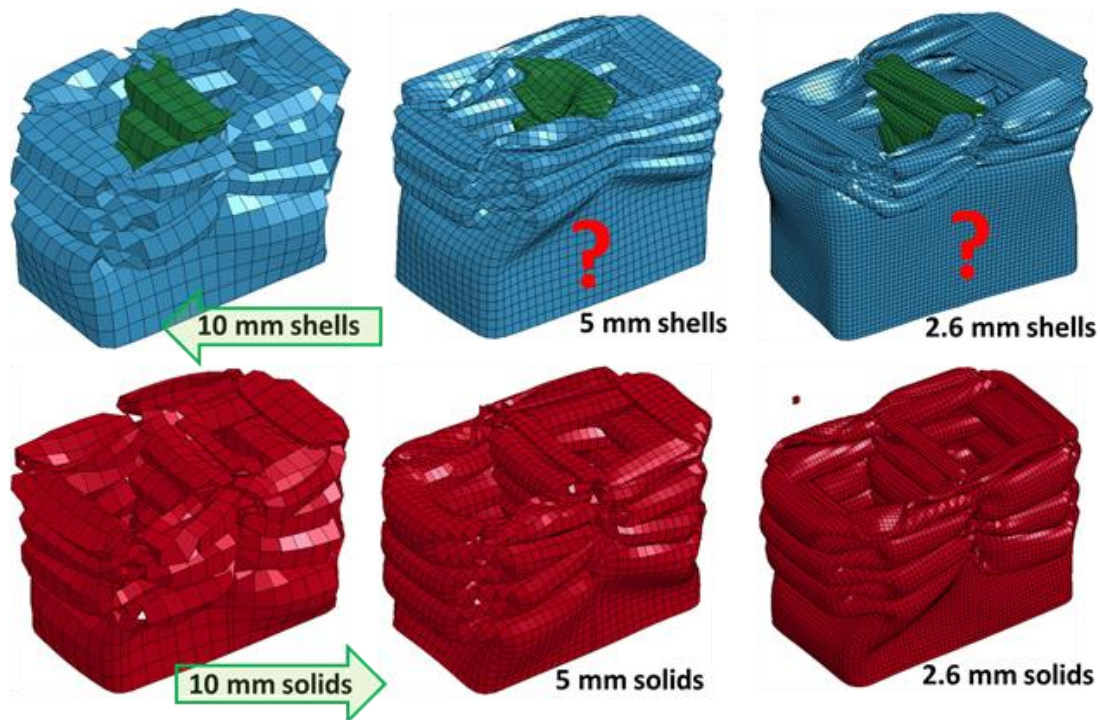


Fig.5: Modelling with shell or solid elements with aspect ratio 4 may be a good starting point.

The two-chamber profile in Figure 2 with initial length 300 mm was compressed 200 mm, and the length of the numerical predictions at right hand side in Figure 5 is therefore about 100 mm. Both the variant with 2.6 mm shell elements and the variant with 2.6 mm solid elements have about 30 elements over the width of each wall that is expected to fold, and these element meshes are both sufficiently fine to illustrate the predicted deformation mode as a relatively smooth surface. The graphical representation looks good for both, and it may therefore be hard to detect if one is not correct. Both these meshes have elements with aspect ratio close to one. The variant with 2.6 mm shell elements predicts folds that are concentrated at the corners, and at least 50 mm of the profile length remains nearly straight. However, the variant with 2.6 mm solid elements predicts folds that are less concentrated at the corners, and about 20 mm of the profile is not included in the deformed portion. The difference between these two alternatives at the right hand side in Figure 5 is sufficiently large to conclude that at least one of them represents a misleading numerical prediction.

The results presented in Figure 1 illustrate an unstable folding mode where especially the details at the T-connection between the mid-wall and the outer skin show large variation. However, the tests show less variation at the other four corners where about 40 mm of the profile length stays more or less straight after testing for six out of eight parallels. This observation corresponds well with the numerical predictions from both meshes at left hand side in Figure 5 where the 10 mm elements have aspect ratio about four. It is also worth noticing that smaller shell elements predicts a mode where the

deformations are too localized into the corners, while the variants based on solid elements seem to be less sensitive with respect to the element size. This means that $\mathbf{ELFORM} = \div 2$ seems able to reduce transverse shear locking for elements that are large compared with the thickness [10] and thereby open for solid elements with aspect ratio in the range 1 – 4 to save computational time in cases where this still means a sufficiently fine mesh to represent the deformation mode. Other authors have observed similar differences between shell- and solid elements, and shell elements with $\mathbf{ELFORM} = 25$ representing through-thickness stretch have shown to raise the force level without predicting the same deformation mode as observed experimentally and with solid elements [11].

5 Numerical modelling guidelines

Both the density and the elastic modulus for aluminium are about one third of these properties for steel, and weigh saving with aluminium is therefore a result of increased thickness and in most cases also somewhat increased cross-section dimensions. It is therefore more likely to end up with solid elements to predict the correct deformation mode and force level for aluminium. However, the increase in computational power during the last decades has opened for smaller elements to represent more details. 5 mm shell elements has become common even in complete car models. This means that even modelling of steel parts with thickness above 1.2 mm may benefit from solid elements. Smaller shell elements may predict local buckling instead of global buckling, and the mistake is hard to detect as the predicted mode looks smooth and realistic. The idea herein is to avoid smaller elements when they do not bring better predictions. A course mesh is ok as it indicates that the predicted deformation mode is questionable, while a fine mesh may indicate trust and should be used with care until it is proved that the model shows convergence towards the correct deformation mode. Figure 6 illustrates larger shell elements as a cost effective alternative where it is visible that the number of elements may be too low to give a proper representation of local folding of for example the tube with diameter 30 times the wall thickness. This tube geometry was found to correspond with one sensitive case in the classification chart by N. Jones [12] where the test result global buckling was related to the initial imperfections. This case has been evaluated with both shell- and solid elements [9], and one result so far is a suggestion with the first three rules for combinations of element types and element meshes that seem able to predict the correct deformation mode:

1. Use elements with aspect ratio about 4 as a starting point for solid and shell elements. Larger elements relative to the thickness require shell elements, while solid elements with $\mathbf{ELFORM} = \div 2$ seem to work well for aspect ratio below 4.
2. Remember that each wall building up a cross-section that is assumed to deform in local buckling should be represented with 8 – 12 elements over the width.
3. It is allowed to use less than 8 elements over the width of each wall as long as the focus is placed on how well this mesh is able to describe the deformation mode.

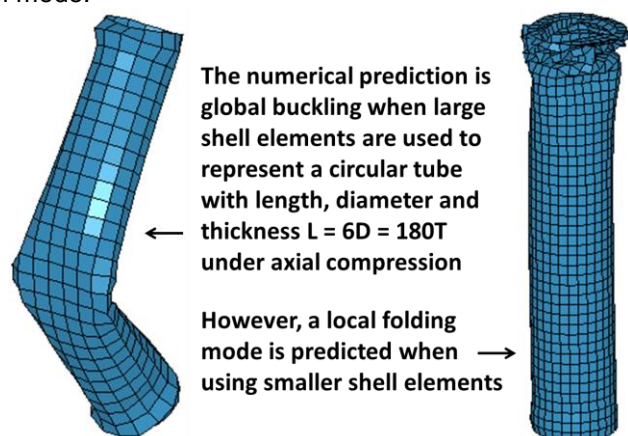


Fig. 6: Global and local buckling as a result of the aspect ratio of the shell elements.

The Belytschko-Tsay shell element does not show convergence when predicting axial crushing, and it is recommended to use 8 – 12 elements over the width of each wall that forms the cross-section [13]. The numerical result in Figure 5 confirms that smaller shell elements than this recommendation may not contribute to a more realistic deformation mode. In the cases shown in Figures 5 and 6, the computational time increases with smaller shell elements that seem to bring the numerical prediction further away from the test results. Eventual increased resources should therefore be prioritised with solid elements to predict smooth surfaces, while large shell elements are ok as it is visible that these predictions are rather rough estimates.

Figure 7 illustrates the effect of the orientation of the solid elements as well as the effect of the relative dimensions of the elements along the main axis [9]. It is likely that solid elements oriented 45° relative to the tube length increases the tendency towards local buckling, and that elements with a somewhat

larger dimension along the tube relative to the dimension over the cross-section may be one way to compensate for this effect. Note that the case with elements oriented 45° had one row of penta elements to finalise each tube end, and the dimension of these six-nodes volume elements was therefore scaled separately. It is currently not concluded whether this numerical uncertainty at the tube ends was caused by reduced stiffness or increased nodal forces when fewer nodes are involved in the contact between the tube and the plates at each end. However, the deformation seems to start at the third row of elements away from the ends, and this indicates that the modelling uncertainties at the tube end are handled sufficiently accurate.

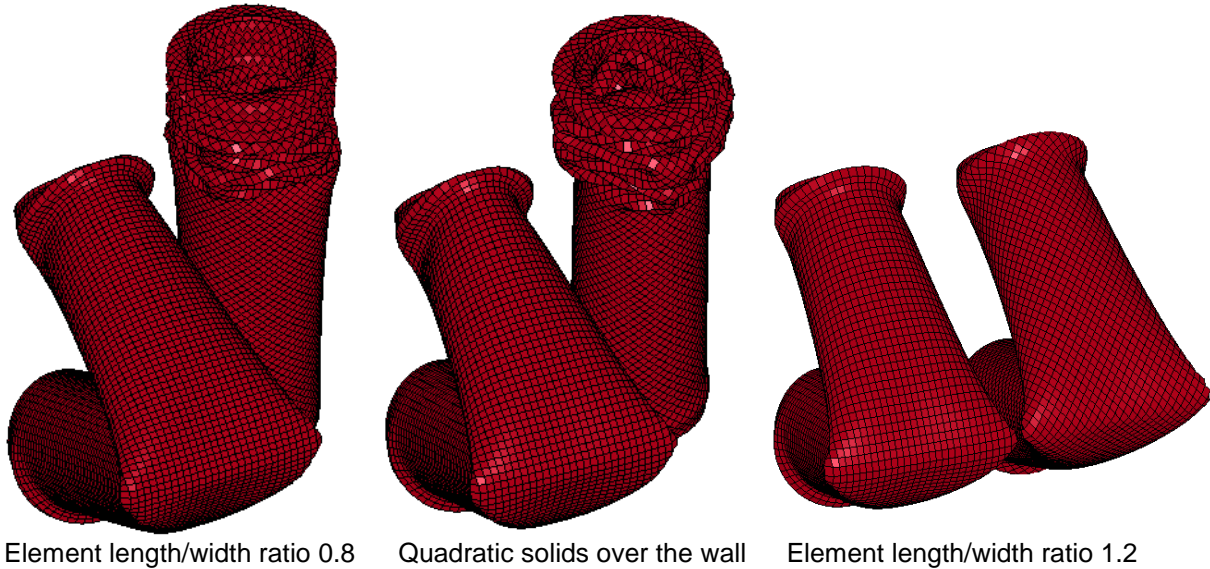


Fig. 7: Effect of element size along the tube relative to the width over the tube cross-section.

Crushing of the two chamber profiles was represented with elements oriented along the main axis. However, in order to fit the cutting angles, some penta elements were added to the hex mesh and some triangular shells replaced some of the four node shells. Figure 5 illustrates the deformation mode where the four corners at the outer skin deform in such a way that the elements get warped similar to the elements oriented 45° when folding the circular tube. Other areas at the two chamber profile display elements that are bended as the elements oriented along the tube main axis. This explains the challenge of predicting the deformation mode when crushing the two chamber profile based on elements where the numerical representation may depend on the orientation of the elements. Moreover, the two T-connections where the mid-wall connects to the outer skin add further complexity. Herein the local representation of the stiffness is important, and the corners have an inner radius adding material that can hardly be represented without a fine solid mesh. The wall thicknesses 1.7 mm and 2.6 mm meet in these T-connections resulting in either varying aspect ratio for the elements or a complex local re-meshing to keep all elements with aspect ratio close to unity.

6 Refinement of the solid mesh with aspect ratio close to unity

The mesh based on solid elements is refined from its starting point with aspect ratio about 4 by keeping one element through the thickness until the aspect ratio is close to 1, see Figure 5. However, the next step with refinement was performed by splitting each hex element into eight new ones as well as each penta element into six new hex elements. The model illustrated in Figure 8 is therefore made with hex elements only. It has two solid elements through the thickness and the "new" nodes in corners are moved after the split to obtain a better representation of the local geometry in the corners. Note that two elements through the wall thickness open for $ELFORM = 1$ that is considerably faster than $ELFORM = \pm 2$. Herein the difference between the predicted deformation modes with these two element formulations may demonstrate that the most simplified alternative with one integration point in the middle displays a more flexible behaviour in the T-connections that connect the mid-wall to the outer skin than the formulation with eight integration points to handle bending. This model is made with elements that are close to cubes geometrically, but the material locally in the corners gets so severely deformed that some of the solid elements become heavily distorted. Therefore, the idea

herein was to investigate to what extent an element formulation that seems able to reduce transverse shear locking for elements that are large compared with the thickness [10] can handle severe deformation when the element changes from a cube initially into something that is far from this.

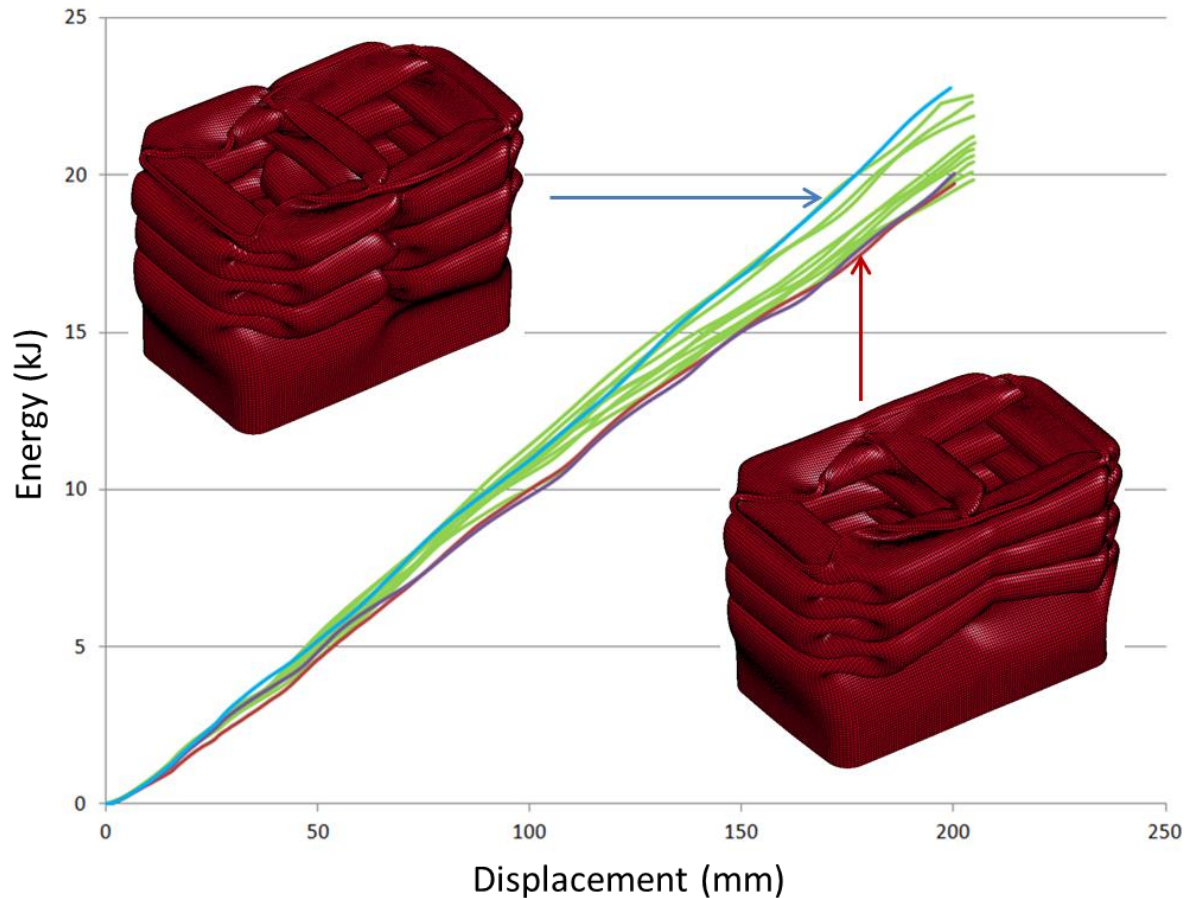


Fig.8: Each solid element is close to a cube that can be split into eight.

The flexibility in the two corners between the mid-wall and the outer skin is important when predicting the deformation mode. Herein it is interesting to notice that the test results seem to be located in between a "flexible T-connection" and a "strict T-connection" represented by **ELFORM 1** and $\div 2$, respectively. The test results in Figure 1 indicate most parallels similar to the variant with lowest energy absorption. But some folds, in for example Test 1 and Test 8, have clearly visible "connections" to the mid-wall. The experiments show tendencies for effective T-connections, and this could partly explain why some of the tests have higher energy absorption than others. However, it is likely that the geometrical imperfections are the most important feature in explaining the uncertainties causing the experimental scatter presented in Figure 1. The cutting angles secure that the folding starts from the top, but the stiffness of the mid-wall and the T-connections is not sufficient to secure progressive folding further down. The mesh is split again and run with ideal geometry and a small imperfection at the top, and the two runs presented in Figure 9 indicates that the cutting angles 12° and 20° make the tested component sensitive to whether the shortest wall starts to fold inwards or outwards. Further work with imperfections was not prioritised as it is better to perform tests with low variation.

From the experiments shown in Figure 1, it is hard to conclude on how many folds that are made at for example the shortest wall. But Test 8 seems to have 3 full folds and this could be similar to Figure 9b, while Test 2 seems to have close to 4 folds at this wall. Also the number of folds at other walls that is displayed in the experiments indicate that the FEM model based on solid elements tend to predict somewhat too large folds, and this situation stays nearly unaffected from the model with two cubic shaped solid element through the thickness to the refined variant with hex element split into 8 new ones. Note that some nodes were moved to improve the representation of local geometry, but the adjustments were relatively small at this stage, and no significant effect was observed.

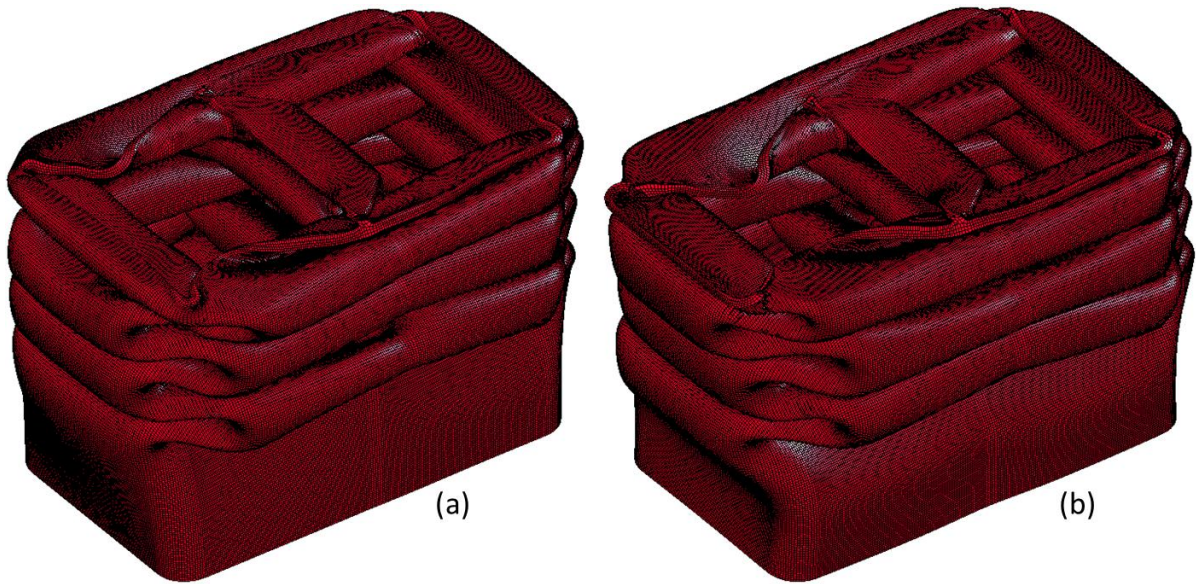


Fig.9: Second split of each hex into eight new ones + adjustments towards aspect ratio 1.

7 Effect of ductility and strain hardening at large strains

The model with small shell elements localise far too much into the corners as seen in Figure 5, but is there some way to get smaller folds with solid elements? As shown in Figure 10a, reduced strain hardening has limited effect, and it cannot be too low as it has to correspond with uniaxial tensile tests and other tests measuring the material response at higher level of strain. Reduced ductility represented by the Cockcroft-Latham parameter may contribute to somewhat smaller folds, but the critical value cannot be too low before the result is more cracks than observed in the tests, see Figure 10b.

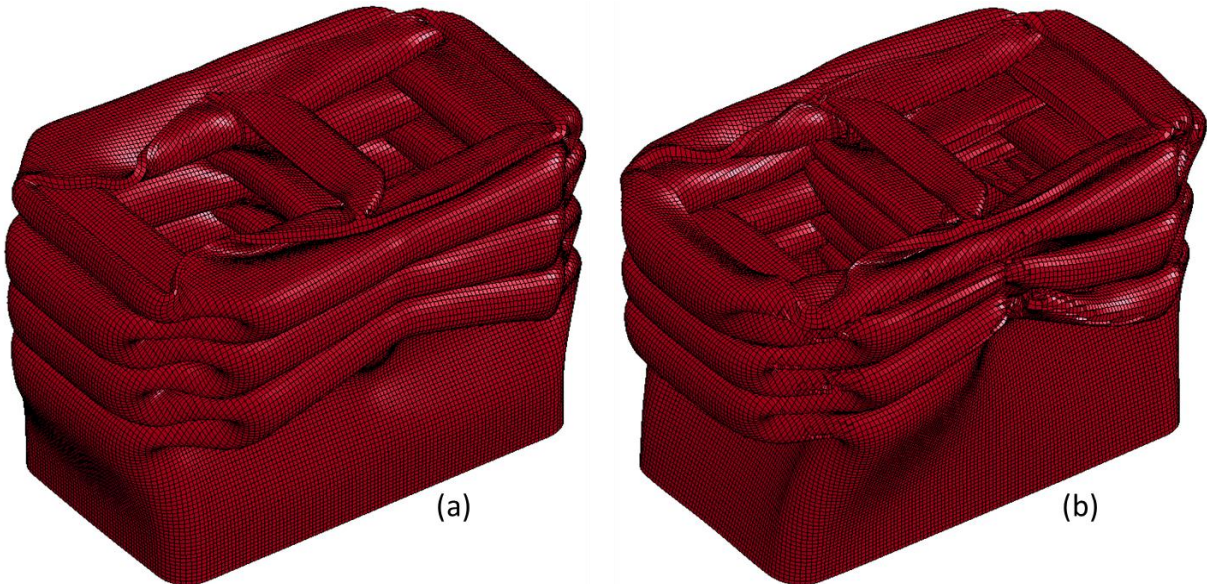


Fig.10: Effect of reduced strain hardening and ductility represented by Cockcroft-Latham.

It is likely that the extruded material shows some local variation that can explain why even parallel tests that are performed with robust profile geometry and triggers that overcome the effect of the geometrical imperfections show some variation. The folding mode may repeat very well resulting in the same strain field as the driver towards fracture, but the cracks are observed at different locations. It is likely that numerical simulations that predict the correct deformation mode are able to detect all positions where a fracture could take place, but the actual cracks are only observed at the positions where severe spots in the strain- and stress fields correspond with locally reduced ductility.

8 Implementation of a shear test from R&D into an industrial environment

The uniaxial tensile test is very useful as it is simple and can be run with many parallels to evaluate the variation in material properties as one important element in the quality control. However, this simple test displays only the first part of the stress-strain curve as the deformation starts to localise inside the area that is under constant deformation until necking. The background herein was the need for measuring the stress-strain curve all the way until fracture, and a shear specimen was developed at the university in Trondheim [14]. This worked well as the specimen had sufficient stiffness to keep the material in place, and the deformation localised into a narrow shear zone where the strain field reached a high maximum value before the specimen went to pieces. However, the specimen geometry was complex, costly to produce and could hardly be used to evaluate local variation. There was a need for implementation into an industrial environment, and this required translation based on proper understanding of the R&D- and the practical situation.

A simple test specimen was made with the central part of the shear test, and the remaining part of the geometry was transformed into a specimen holder [8]. It was then possible to perform the shear test with a simple specimen with automatic mounting of the extensometers. The laboratory personnel were involved in the implementation process to secure that the shear test could be performed in the same way as the uniaxial tensile test. Remember that the last measurement is limited to the point where the remaining capacity to tear off the specimen is equal to the elastic energy in the test arrangement. It is therefore beneficial to have at test setup with large stiffness to minimise the elastic deformation outside a relatively narrow area that is tested. It is also important to model the test specimen with a combination of element type, element orientation and element mesh that is able to predict the correct deformation mode, and herein cubic shaped solid element with dimension about 0.1 mm is required to capture a reasonable critical value for the Cockcroft-Latham parameter, see Figure 11.

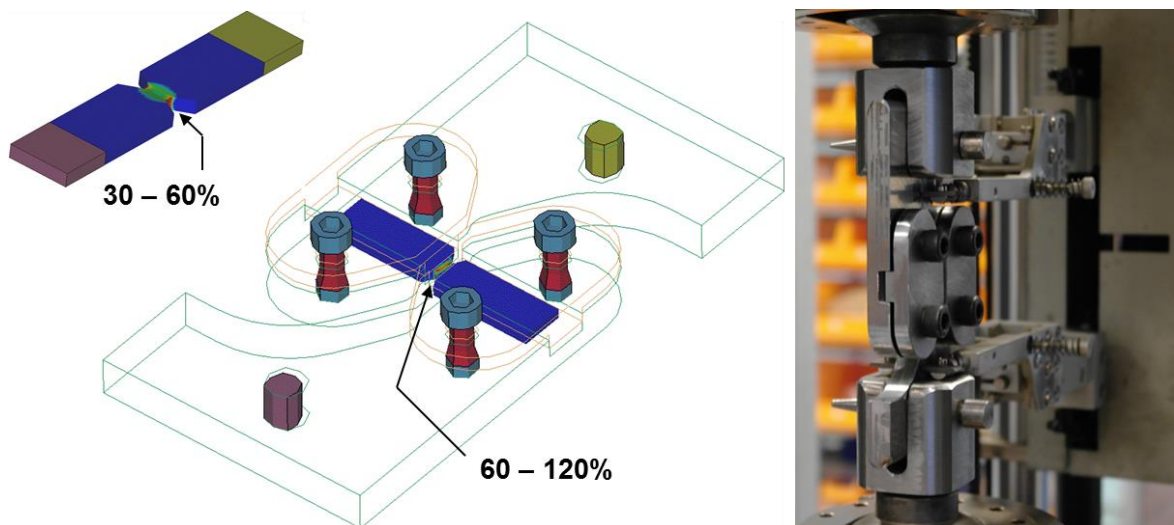
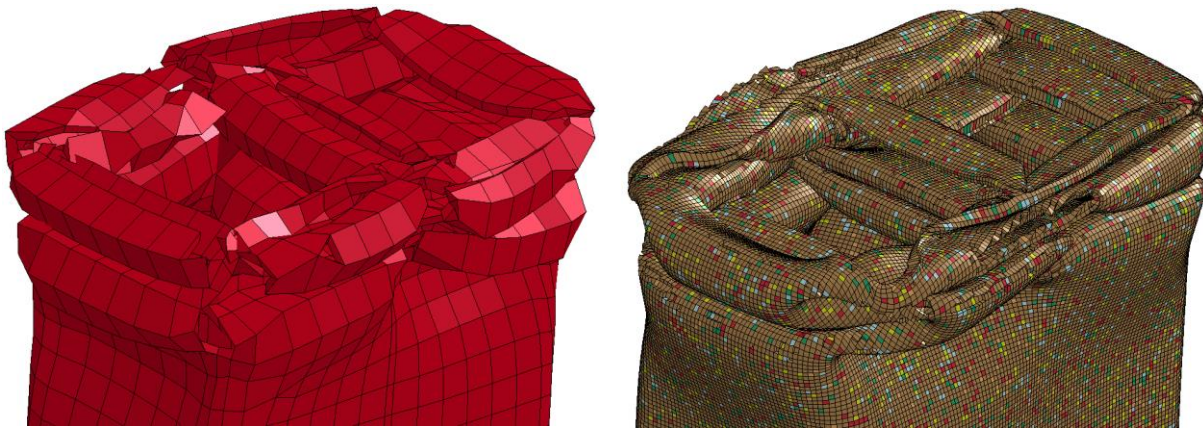


Fig. 11: Inverse modelling of a simple specimen where a holder applies shear loading into it.

It is interesting to notice that the shear test may show anisotropy for both force-displacement curves and displacement at fracture when the specimens are taken with different orientation relative to the extrusion direction. The result is then an anisotropic yield surface that together with Cockcroft-Latham seems to capture this [8]. However, most structural components have more flexibility to deform, and the anisotropy is often less important for realistic product geometries. The deformation mode is likely to be determined by the stiffness offered by the geometry, and the influence from some anisotropy is less important when it comes to the effects that determine the deformation mode for real product geometries. It is often better to prioritise elements to handle the correct deformation mode than to allocate most of the resources into advanced material models that require a lot of calibration work. It is likely that **MAT_107** can be a good alternative, see Figure 12. Complete car simulations may require elements with aspect ratio about 4 and some reduction of the critical Cockcroft-Latham value, while other applications requires a fine solid mesh and local variation in material properties. Note that the numerical predictions in Figure 12 were run with somewhat reduced Cockcroft-Latham values to predict more cracks, and the status is shown where the first two folds are made.



10 mm solid elements

Refined mesh and local variation in material properties

Fig. 12: The details are not captured but practical engineers may still prefer 10 mm elements.

9 Summary

This study shows that a simple material model like MAT_107 seems to work well together with a combination of element type and mesh that predict the correct deformation mode. The Cockcroft-Latham value from inverse modelling can be used directly for solid elements with aspect ratio about one, while a reduced critical value correspond with larger elements. The results show that the relatively thin mid-wall struggle to secure progressive folding for this two-chamber profile, and within the tolerances a more robust folding mode is likely for a profile variant with thickness 2.25 mm for all walls. Reduced cutting angles will also contribute to less experimental variation. The benefit from keeping the material model as simple as possible is reduced cost by calibration based on a simple test specimen and a specimen holder to run the shear test in the same way as a uniaxial tensile test [8].

10 Literature

- [1] Kojima, S., Yasuki, T., Mikutsu, S., Takatsudo, T.: "A Study on Yielding Function of Aluminium Honeycomb", 5th European LS-DYNA Users Conference, Birmingham, UK, 2005.
- [2] Tryland, T.: "Alternative Model of the Offset Deformable Barrier", 4th LS-DYNA Forum, Bamberg, Germany, 2005.
- [3] Tryland, T.: "A Simple Compression Test to Evaluate Ductility", 9th Nordic LS-DYNA Users Forum, Gothenburg, Sweden, 2008.
- [4] Olsson, B.: "Testing of Constitutive Models of AA6082-T6 in LS-DYNA", Nordic LS-DYNA Users Forum 2014, Gothenburg, Sweden, 2014.
- [5] Tryland, T., Larsen, P. K. and Langseth, M.: "Design of I-Beams and Deck Profiles under Concentrated Loading", Journal of Structural Engineering, Vol. 130, No. 3, March 2004.
- [6] BS 8118.: "Structural use of aluminium. Part 1. Code of practise for design", Civil Engineering and Building Structures Standards Policy Committee, ISBN 0-580-19209-1, 1991.
- [7] Eurocode 9.: "Eurocode 9: Design of aluminium structures – Part 1.1 General rules and rules for buildings", prENV 1999-1-1, CEN, European Committee for Standardization, 2007.
- [8] Tryland, T., Berstad, T.: "A Simple Shear Test to Evaluate Material Ductility based on Specimens Cut from thin-Walled Sections", 11th LS-DYNA Forum, Ulm, Germany, 2012.
- [9] Tryland, T.: "Combinations of Meshes and Elements that seems able to Predict the Correct Deformation Mode", 13th LS-DYNA Forum, Bamberg, Germany, 2014.
- [10] Borrvall, T.: "A heuristic attempt to reduce transverse shear locking in fully integrated hexahedra with poor aspect ratio", 7th European LS-DYNA Conference, Salzburg, 2009.
- [11] Fyllingen, Ø., Hopperstad, O.S., Hansen, A.G., Langseth, M.: "Brick versus shell elements in simulations of aluminium extrusions subjected to axial crushing", 7th European LS-DYNA Conference, Salzburg, 2009.
- [12] Jones, N.: "Structural impact", Cambridge University Press, 1989, Figure 9.32.
- [13] Du Bois, P.: "Crashworthiness Engineering with LS-DYNA", Notes, Hermes Engineering, 1999.
- [14] Achani, D.: "Constitutive models of elastoplasticity and fracture for aluminium alloys under path change", PhD thesis, Department of Structural Engineering, Norwegian University of Science and Technology, NTNU, Trondheim, ISBN 82-471-7902-2, page 133-135, 2006.